

# Electron-phonon coupling and optical transitions for indirect-gap semiconductor nanocrystals

C. Delerue,<sup>1,\*</sup> G. Allan,<sup>1</sup> and M. Lannoo<sup>2</sup>

<sup>1</sup>*Institut d'Electronique et de Microélectronique du Nord (UMR CNRS 8520), Département Institut Supérieur d'Electronique du Nord, 41 boulevard Vauban, 59046 Lille Cédex, France*

<sup>2</sup>*Laboratoire Matériaux et Microélectronique de Provence, Institut Supérieur d'Electronique de la Méditerranée, Place Georges Pompidou, 83000 Toulon, France*

(Received 5 June 2001; published 12 October 2001)

We show that it is possible to perform full microscopic calculations of the phonon-assisted and no-phonon radiative transitions in silicon nanocrystals. These are based on a tight-binding Hamiltonian for the electron and electron-phonon part together with a valence force-field model for phonons. We predict an unexpected large broadening of the luminescence peaks attributed to the breaking of bulk selection rules and to multiphonon effects in the acoustic range. We also find that phonon-assisted transitions dominate over the full range of sizes. These results are compared to previous estimates in the effective-mass approximation and are used to discuss available experimental data.

DOI: 10.1103/PhysRevB.64.193402

PACS number(s): 78.67.Bf, 78.55.Ap

Quantum dots (QD's) can be considered as artificial atoms since their electronic spectrum consists of discrete atomiclike energy levels. Indeed when they are built from direct-gap semiconductors, their low-temperature photoluminescence (PL) is mainly characterized by sharp spikes with linewidth lower than a few hundreds of  $\mu\text{eV}$ , confirming the atomiclike nature of the emitting state.<sup>1</sup> The situation becomes more complex for QD's made from indirect-gap semiconductors like silicon. The reason is that purely electronic optical transitions in the gap region are strictly forbidden in the bulk ( $\mathbf{k}$  selection rule) and only phonon-assisted transitions can exist. In the corresponding QD's however the  $\mathbf{k}$  selection rule is broken<sup>2</sup> and there is a size-dependent competition between no-phonon and phonon-assisted transitions. This has been confirmed for nanocrystalline porous silicon<sup>3</sup> where several experimental studies<sup>4-6</sup> show that phonon-assisted transitions remain efficient. On the theoretical side there only exists one model calculation due to Hybertsen<sup>7</sup> based on simple effective-mass approximation (EMA) that is too crude for small QD's.<sup>8</sup>

There is thus need for a more quantitative approach to these electron-phonon related phenomena. Due to its complexity, such a calculation is far beyond the present possibilities of *ab initio* theories for the range of interesting crystals sizes (several nanometers). Our aim is to demonstrate that it becomes feasible when using well-established semiempirical techniques like tight-binding (TB) and a valence force-field model. We consider ideal hydrogenated silicon clusters and present results concerning the size dependence of the broadening of optical spectra and the relative strength of phonon-assisted and no-phonon transitions. Contrary to what is usually assumed we find that, for gap energies larger than 1.5 eV, multiphonon effects in the low acoustic range become important and contribute to the broadening of the spectral lines. Finally, our results are used to give a plausible interpretation of the various experimental data of Refs. 6 and 9.

The TB parameters are those discussed in Ref. 8 and provide a band gap size in good agreement (within  $\sim 0.1$  eV) with previous works.<sup>2,10</sup> The vibrational modes of the QD's are calculated using a valence force-field model<sup>11</sup> that pro-

vides a very good fit to the phonon-dispersion curves of bulk silicon. Finally, for each QD, we calculate the radiative recombination rate  $W(h\nu)$  of photons  $h\nu$  as follows. We start from the usual expression for the dipolar transition:<sup>8</sup>

$$W(h\nu) = K \sum_{i,f} p(i) |\langle \Psi_i | \mathbf{p} | \Psi_f \rangle|^2 \quad (1)$$

with  $K = 48\pi^2 e^2 n \nu / \hbar m^2 c^3$ .  $|\Psi_i\rangle$  and  $|\Psi_f\rangle$  are, respectively, initial and final states of the system with energy  $E_i = E_f + h\nu$ ,  $p(i)$  is the probability of occupation of the initial state and  $n$  is the refractive index. The wave functions include the coordinates of the electrons and nuclei. Working within the adiabatic approximation, the matrix element of the momentum in (1) becomes

$$\langle \Psi_i | \mathbf{p} | \Psi_f \rangle = \langle \chi_i | \langle \psi_i | \mathbf{p} | \psi_f \rangle | \chi_f \rangle, \quad (2)$$

$|\chi_i\rangle$  and  $|\chi_f\rangle$  are the vibrational states of the system that are built in the harmonic approximation from independent harmonic oscillators corresponding to each normal mode  $Q_j$ . These oscillators are centered on the equilibrium configurations of the nuclei that are not the same in the excited state and in the ground state. This is due to the lattice relaxation in the excited state induced by the transfer of an electron from a valence state to a conduction state that tends to deform the lattice.<sup>8</sup> Thus, for each mode  $Q_j$  the electronic energies of the excited state ( $\varepsilon_i$ ) and of the ground state ( $\varepsilon_f$ ) are parabolic functions centered, respectively, on  $Q_j^i$  and  $Q_j^f$ .  $|\psi_i\rangle$  and  $|\psi_f\rangle$  in Eq. (2) are the electronic wave functions that can be defined for any set of nuclear coordinates.<sup>12</sup> Because each normal mode gives a contribution of order  $1/\sqrt{3N}$  (Ref. 12) ( $N$  is the number of atoms), we expand the matrix element (2) to first order in the normal modes:

$$\langle \Psi_i | \mathbf{p} | \Psi_f \rangle = \langle \psi_i | \mathbf{p} | \psi_f \rangle_0 \langle \chi_i | \chi_f \rangle + \sum_{j=1}^{3N} \mathbf{A}_j \langle \chi_i | Q_j - Q_j^f | \chi_f \rangle \quad (3)$$

where  $\mathbf{A}_j = (\partial \langle \psi_i | \mathbf{p} | \psi_f \rangle / \partial Q_j)_0$ . The index 0 means that the quantities are calculated at the equilibrium positions of the

final state. We now use the fact that the vibrational states are products of  $3N$  harmonic oscillators:

$$\langle \chi_i | \chi_f \rangle = \prod_{j,j'=1}^{3N} \langle i, n_j | f, n_j' \rangle \quad (4)$$

where  $n_j(n_j')$  is the number of phonons in mode  $j(j')$ . The overlaps between two displaced harmonic oscillators can be expressed in terms of the quantities  $V_j$ :<sup>12</sup>

$$V_j = -\sqrt{\omega_j/2\hbar}(Q_j^f - Q_j^i) = \sqrt{1/2\hbar\omega_j^3} \left[ \frac{\partial}{\partial Q_j} (\varepsilon_f - \varepsilon_i) \right]_0 \quad (5)$$

where  $\hbar\omega_j$  is the phonon energy in the mode  $j$ . Noticing that the quantities  $V_j$  are of the order  $1/\sqrt{3N}$ , we have<sup>12</sup>

$$\langle i, n_j | f, n_j \rangle \approx 1 - (n_j + 1/2)S_j$$

$$\langle i, n_j | f, n_j + 1 \rangle \approx \sqrt{n_j + 1} V_j \quad (6)$$

$$\langle i, n_j | f, n_j - 1 \rangle \approx -\sqrt{n_j} V_j$$

where the quantities  $S_j$  are the so-called Huang-Rhys factors  $S_j = V_j^2$ .<sup>12</sup> All the other overlaps are of higher order. Using Eq. (6) and the transformation  $Q_j - Q_j^f = \sqrt{\hbar/2\omega_j}(a_{jj}^+ + a_{jj})$  in terms of the creation and annihilation operators and averaging over  $n_j$ , we obtain the following recombination rates after straightforward algebra:

$$\text{no phonon: } W_{\text{nop}} \approx K \left| \langle \psi_i | \mathbf{p} | \psi_f \rangle_0 + \sum_{j=1}^{3N} \sqrt{(\hbar/2\omega_j)} V_j \mathbf{A}_j \right|^2 \quad (7)$$

$$\text{one-phonon emission } (\hbar\omega_j): W \approx K \left| \langle \psi_i | \mathbf{p} | \psi_f \rangle_0 V_j + \sqrt{(\hbar/2\omega_j)} \mathbf{A}_j^2 \{\bar{n}_j + 1\} \right|^2 \quad (8)$$

$$\text{one-phonon absorption } (\hbar\omega_j): W \approx K - \left| \langle \psi_i | \mathbf{p} | \psi_f \rangle_0 V_j + \sqrt{(\hbar/2\omega_j)} \mathbf{A}_j^2 \bar{n}_j \right|^2 \quad (9)$$

where  $\bar{n}_j = [\exp(\hbar\omega_j/kT) - 1]^{-1}$ . The heavy part of the work is the evaluation of the coupling coefficients  $\mathbf{A}_j$  and  $V_j$  that are calculated numerically for *each* mode  $j$  of the QD. The optical matrix elements are calculated like in Ref. 13 and the matrix elements of the Hamiltonian are made dependent on the atomic positions following the rules of Ref. 14.

Figure 1 shows the recombination rates at 4 K calculated for a 2.85 nm diameter QD with respect to the energy of the phonons involved in the transitions. At this temperature, the

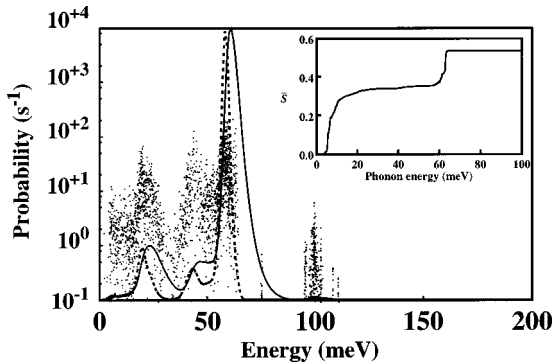


FIG. 1. Radiative recombination rate at 4 K (+) with respect to the energy of the phonon involved in the transition for a 2.85 nm hydrogen-passivated QD. The dotted line shows in arbitrary units the single cluster PL intensity assuming it is directly proportional to the recombination rate, neglecting acoustic phonons. The full line shows the PL intensity including the broadening by the multiphonon effect. The insert shows  $\bar{S}(\hbar\omega)$  as a function of the phonon energy.

phonon absorption process is negligible and the recombination proceeds by phonon emission. We also plot on Fig. 1 the PL spectrum below the no-phonon line calculated assuming that the PL intensity is directly proportional to the recombination rate. It shows, in agreement with the EMA results of Ref. 7, that optical modes dominate and that the contributions from TA modes are smaller. However, there is a problem associated with the direct use of Eqs. (8) and (9) to calculate line shapes. This is connected with the fact that the total Huang-Rhys factor  $\bar{S} = \sum_j (2\bar{n}_j + 1)S_j$  increases rapidly with decreasing size (like  $N^{-1}$ ) and reaches a value close to 1 for band gaps around 2 eV that means that multiphonon processes become important.<sup>12</sup> From this point of view it is interesting to analyze the quantity  $\bar{S}(\hbar\omega)$  that is the sum of all  $S_j$  with  $\hbar\omega_j < \hbar\omega$ . Figure 1 shows that  $\bar{S}(\hbar\omega)$  has essentially two contributions: one originating from low-frequency acoustical modes ( $\hbar\omega < 15$  meV) and a smaller one from the highest optical modes. The first one intuitively corresponds to relaxation effects in the excitonic state, analyzed in Ref. 8. All this means that for small silicon QD's formulas (7)–(9) are no more valid.

The way to handle this problem can be easily analyzed at  $T=0$  K where only the processes given by Eqs. (7) and (8) subsist. For the low acoustical modes we find that terms in  $\mathbf{A}_j$  are negligible so that we only retain terms in  $V_j$  that result from the overlap factors. Thus each process given by Eqs. (7) and (8) has replica corresponding to the emission of  $p$  phonons whose intensity is proportional to the total overlap between these acoustical modes, which using Eq. (6) can be written as

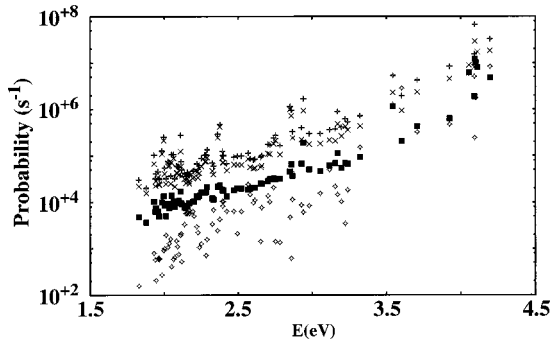


FIG. 2. Recombination rate as a function of the QD band gap: sum of no-phonon and phonon-assisted processes (+); no phonon (■); transitions assisted by optical phonons (×); by TA phonons (●).

$$\prod_{k=1}^p S_k \prod_{l=1}^{N_a-p} (1-S_l), \quad (10)$$

where  $N_a$  is the total number of low acoustic modes. As in Ref. 12 we now consider that the acoustic modes of interest are degenerate at  $\hbar\omega_a \sim 10$  meV that according to the inset of Fig. 1 should be an excellent approximation. Summing all independent contributions (10) at fixed  $p$  gives, for  $p \ll N_a$  and  $S_l \ll 1$ , a total relative intensity  $I_p = (\bar{S}^p/p!) \exp(-\bar{S}_a)$  where  $\bar{S}_a$  is the sum of all  $S_k$  for these modes. This means that Eqs. (7) and (8) are still valid but have replica at  $p\hbar\omega_a$  with relative intensity  $I_p$ . In other words the peaks corresponding to Eqs. (7) and (8) have to be broadened by the spectral function  $I_p$ . This procedure directly applies to our case ( $T=4$  K), but can be extended to higher temperature by use of Bessel functions as shown in Ref. 12.

Figure 1 shows that the multiphonon broadening by the low acoustical modes is substantial so that the total broadening is large, of the order of 10's of meV for crystallites with 3 nm diameter. Thus the PL of small silicon QD's (below 4 nm) should not correspond to sharp spikes as for QD's made of direct-gap semiconductors. Another important result of our calculations is the relative strength of no-phonon and phonon-assisted transitions. These are plotted in Fig. 2 where one sees that phonon-assisted transitions dominate over the whole range of sizes. We also obtain that the ratio of transition rates for one-phonon acoustical  $W_{ac}$  and optical processes  $W_{opt}$  is  $W_{opt}/W_{ac} \sim 10$ .

Our results confirm some points of the EMA calculation of Ref. 7: (i) the validity of the neglect of transverse acoustic processes, (ii) the order of magnitude of phonon-assisted processes with radiative rate  $W \sim 10^4 - 10^5/\text{sec}$  for gaps in the 1.8–2 eV range. On the other hand the no-phonon rates  $W_{nop}$  are more difficult to compare due to strong oscillations vs size. Our values seem nevertheless consistently smaller by a factor of order less than 10 probably due to simplifications arising in the EMA treatment. Comparison with experiment is more delicate since our calculations correspond to ideal hydrogen-terminated crystals. The closest experimental situation corresponds to the recent study of alkyl-terminated silicon crystal of Ref. 9 that supports our findings: agreement

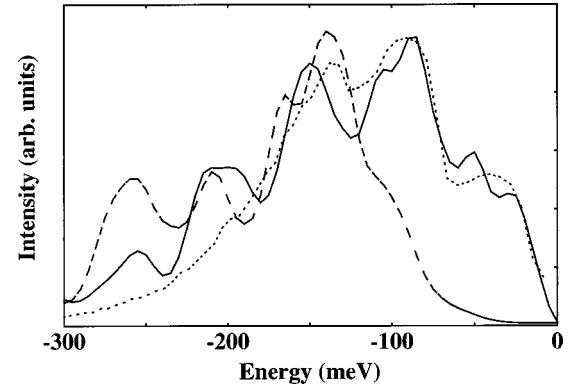


FIG. 3. Experimental resonant PL spectrum for an excitation energy equal to 1.9 eV (full line) (Ref. 19) compared to the theoretical result for a hydrogen-passivated cluster without (dashed line) or with (dotted line) enhancement of the no-phonon transition.

for the gap vs size but also the fact that phonon-assisted transitions dominate even for the smaller crystallites.

The comparison with the resonant PL experiments of Kovalev *et al.*<sup>6</sup> performed on oxidized porous silicon is much less direct. Indeed it is well known that large strains occur at the Si-SiO<sub>2</sub> interface resulting in some cases in the creation of surface defects like the Si=O defect<sup>15</sup> or self-trapped excitons.<sup>16</sup> The situation then becomes quite different from our ideal hydrogenated Si crystallite. Let us nevertheless try to make the comparison between the results of Ref. 6 and those of Fig. 2. This leads to two conclusions: (i) the calculation gives  $W_{opt}/W_{ac} \sim 10$  in full agreement with experiment; (ii) on the contrary, for gaps in the 1.8–2 eV range, our predicted values for  $W_{nop}/W_{opt}$  are about 150 times smaller (note however that there are strong oscillations in the theoretical values that can be larger than one order of magnitude). The origin of such a difference must then be ascribed to the existence of strained interface regions in the oxidized samples. However it cannot be due to the deep defects mentioned earlier (self-trapped exciton, Si=O) since their Stokes shift is by far too large<sup>15,16</sup> to be observable in resonant PL. One must then look for states with weaker localization due to more or less distorted bonds in the vicinity of the interface region. This is quite similar to what happens in theoretical descriptions of amorphous silicon. We have shown recently<sup>17</sup> that such distorted bonds are responsible for the band tails of localized states of *a*-Si that can extend over regions containing 10–100 atoms. Furthermore we have calculated the corresponding radiative recombination rates that turn out to be in the  $10^5 - 10^6/\text{sec}$  range,<sup>18</sup> i.e.,  $\sim 100$  times larger than our values for ideal clusters.

To strengthen this conclusion let us use a simple EMA argument. We consider a strained region resulting in a parabolic like central potential, attractive for electrons  $e$  and holes  $h$ . This results in localized states with Gaussian envelope functions  $\psi_e = \psi_h = \exp(-\alpha r^2)$ ,  $r$  being the distance from the potential extrema. We now use the argument developed in Ref. 7 that the zero-phonon and phonon-assisted processes, respectively, scale as  $I_0 = |\int \psi_e \psi_h e^{i\mathbf{k}_0 \cdot \mathbf{r}} dv|^2$  (where  $\mathbf{k}_0$  is the wave vector of one of the conduction band minima) and  $I_1 = \int |\psi_e|^2 |\psi_h|^2 dv$ . We obtain  $I_0 = \exp(-k_0^2/4\alpha)$  and  $I_1$

$=(\alpha/2\pi)^{3/2}$ . In fact  $I_1$  represents a measure of  $\Omega^{-1}$  where  $\Omega$  is the volume over which the localized state extends (the same definition was used for  $\alpha$ -Si in Ref. 17. We can inject the value  $\alpha=2\pi\Omega^{-2/3}$  to calculate  $I_0$  vs  $\Omega$ . From Ref. 7  $I_0$  represents  $W_{\text{nop}}$  in units of the rate for direct transitions, i.e.,  $10^9/\text{sec}$ . We thus get

$$W_{\text{nop}} \approx 10^9/\text{sec} \exp\left(-\frac{k_0^2}{8\pi}\Omega^{2/3}\right) \quad (11)$$

which, for states localized on  $\sim 100$  atoms, give a value of order  $10^6/\text{sec}$  exactly in the range calculated in Ref. 18 for  $\alpha$ -Si.

Our view of the resonant PL of oxidized nanocrystals is thus that it is dominated by such transitions between localized states due to strained bonds. As discussed before  $W_{\text{nop}}$  is drastically increased taking values much larger than for our ideal clusters. On the other hand this localization of the states does not affect the one-phonon rates too much since they only vary as  $\Omega^{-1}$ . To confirm this point of view we have thus calculated the resonant PL spectrum for one QD of size

2.85 nm and gap 1.83 eV, and compared it to unpublished results<sup>19</sup> of the authors of Ref. 6. These are obtained for a sample with non resonant PL centered at 2.2 eV, the resonant PL being excited on the low-energy side at 1.9 eV. To get a meaningful resonant PL spectrum we proceed in two steps: (a) we calculate the gap dependence of each individual spectrum as resulting from a simple shift of the level structure obtained for the QD of gap 1.83 eV; (b) we convolute this by the gap-distribution function taken from the nonresonant PL of Ref. 6 under the form of a Gaussian reproducing correctly the low-energy side near 1.9 eV. The result of this procedure is plotted on Fig. 3. This shows that the predicted curve with  $W_{\text{nop}}$  calculated for the ideal QD does not compare well with experiment. On the other hand if the relative value of  $W_{\text{nop}}$  is increased by a factor  $\sim 150$  then the agreement becomes strikingly good.

In conclusion we have shown that it is possible to perform microscopic calculations of the optical spectrum due to phonon-assisted transitions in silicon crystallites of size up to 3 nm. We show that these always dominate over no-phonon transitions.

\*Email address: delerue@isen.fr

<sup>1</sup>K. Brunner, G. Abstreiter, G. Bohm, G. Trankle, and G. Weimann, Phys. Rev. Lett. **73**, 1138 (1994); S. A. Empedocles, D. J. Norris, and M. G. Bawendi, *ibid.* **27**, 3873 (1996); D. Gammon, E. S. Snow, B. V. Shanabrook, D. S. Katzer, and D. Park, *ibid.* **76**, 3005 (1996).

<sup>2</sup>C. Delerue, G. Allan, and M. Lannoo, Phys. Rev. B **48**, 11 024 (1993).

<sup>3</sup>For a recent review, see A. G. Cullis, L. T. Canham, and P. D. J. Calcott, J. Appl. Phys. **82**, 909 (1997).

<sup>4</sup>P. D. J. Calcott, K. J. Nash, L. T. Canham, M. J. Kane, and D. Brumhead, J. Phys.: Condens. Matter **5**, 91 (1993); T. Suemoto, K. Tanaka, A. Nakajima, and T. Itakura, Phys. Rev. Lett. **70**, 3659 (1993).

<sup>5</sup>L. Brus, in *Light Emission in Silicon. From Physics to Devices*, edited by D. Lockwood, Semiconductors and Semimetals, Vol. 49 (Academic Press, New York, 1998), p. 303.

<sup>6</sup>D. Kovalev, H. Heckler, M. Ben-Chorin, G. Polisski, M. Schwartzkopff, and F. Koch, Phys. Rev. Lett. **81**, 2803 (1998).

<sup>7</sup>M. S. Hybertsen, Phys. Rev. Lett. **72**, 1514 (1994).

<sup>8</sup>E. Martin, C. Delerue, G. Allan, and M. Lannoo, Phys. Rev. B **50**, 18 258 (1994).

<sup>9</sup>H. W. Lee, P. A. Thielen, B. R. Taylor, G. R. Delgado, S. M.

Kauzlarich, and C.-S. Yang, in *Microcrystalline and Nanocrystalline Semiconductors-2000*, edited by P.M. Fauchet, J. M. Buriak, L. T. Canham, N. Koshida, and B. E. White, Jr., (Mat. Res. Soc. Proc. **638**, Pittsburgh, PA, 2001).

<sup>10</sup>L. W. Wang and A. Zunger, J. Phys. Chem. **98**, 2158 (1994).

<sup>11</sup>R. Tubino, L. Piseri, and G. Zerbi, J. Chem. Phys. **56**, 1022 (1972); D. Vanderbilt, S. H. Taole, and S. Narasimham, Phys. Rev. B **40**, 5657 (1989).

<sup>12</sup>K. Huang and A. Rhys, Proc. R. Soc. London, Ser. A **204**, 406 (1950); J. C. Bourgoin and M. Lannoo, in *Point Defects in Semiconductors II, Experimental Aspects*, Springer Series in Solid-State Sciences, Vol. 35 (Springer, Berlin, 1981), p. 103.

<sup>13</sup>J. Petit, G. Allan, and M. Lannoo, Phys. Rev. B **33**, 8595 (1986).

<sup>14</sup>W. A. Harrison, *Electronic Structure and the Properties of Solids* (Freeman, San Francisco, 1980).

<sup>15</sup>M. V. Wolkin, J. Jorne, P. M. Fauchet, G. Allan, and C. Delerue, Phys. Rev. Lett. **82**, 197 (1999).

<sup>16</sup>G. Allan, C. Delerue, and M. Lannoo, Phys. Rev. Lett. **76**, 2961 (1996).

<sup>17</sup>G. Allan, C. Delerue, and M. Lannoo, Phys. Rev. B **57**, 6933 (1998).

<sup>18</sup>G. Allan, C. Delerue, and M. Lannoo, Phys. Rev. Lett. **78**, 3161 (1997).

<sup>19</sup>D. Kovalev (unpublished).